PFG 2010 / 6, 463 – 474
Stuttgart, Dezember 2010

Article

Curvelet-based Change Detection on SAR Images for Natural Disaster Mapping

Andreas Schmitt, Birgit Wessel & Achim Roth, Oberpfaffenhofen

Keywords: SAR, Change Detection, Alternative Image Representation, Curvelets

Summary: This paper focuses on the use of SAR data in the context of natural disasters. A Curvelet-based change detection algorithm is presented that automatically extracts changes in the radar backscattering from two TerraSAR-X acquisitions – pre-disaster and post-disaster – of the same area. After a logarithmic scaling of the geocoded amplitude images the Curvelet-transform is applied. The differentiation is then done in the Curvelet-coefficient domain where each coefficient represents the strength of a linear structure apparent in the original image. In order to reduce noise the resulting coefficient differences are weighted by a special function that suppresses minor, noise-like structures. The resulting enhanced coefficients are transformed back to the image domain and brought to the original scaling, so that the values in the difference image describe the increase and the decrease with respect to the amplitude value in the initial image. This approach is applied on three crisis scenarios: flood, forest fire, and earthquake. For all scenarios including natural landscapes and urban environments as well areas with changes in the radar amplitude are clearly delineated. The interpretation of the changes detected in the radar images needs additional knowledge, e. g., pre-disaster maps. The combination of both could possibly deliver a robust and reliable database for the coordination of rescue teams after large-scale natural disasters.

Zusammenfassung: *Auf Curvelets basierende Änderungserkennung in SAR-Bildern für die Kartierung von Naturkatastrophen.* Fernerkundung im Krisenkontext basiert auf einer schnellen und zuverlässigen Datenakquisition. Radarsysteme sind für diesen Zweck aufgrund ihrer i. A. wetter- und beleuchtungsunabhängigen Aufnahme besonders geeignet. In diesem Artikel wird eine Methode vorgestellt, aus zeitlich versetzten Aufnahmen des deutschen Radarsatelliten TerraSAR-X vollautomatisch Veränderungen abzuleiten. Die geokodierten Radaramplitudenbilder werden dazu logarithmisch skaliert und mithilfe der Curvelet-Transformation in den Curvelet-Koeffizientenraum überführt. Jeder Koeffizient entspricht hier der Stärke einer bestimmten linearen Struktur im Bild. Aus den Koeffizienten zweier Bilder kann nun ein Differenz-Koeffizientenbild berechnet und anschließend durch eine spezielle Gewichtungsfunktion verbessert werden. Während starke Strukturen unverändert übernommen werden, erfolgt für Strukturen mittlerer Stärke eine kontinuierliche Herabgewichtung bis zum kompletten Entfernen zu schwacher Strukturen. Auf diese Weise wird nicht nur die Anzahl der Koeffizienten, sondern auch das Rauschen im Bild deutlich verringert und der Bildinhalt auf die wichtigsten Strukturen beschränkt. Nach der Rücktransformation in den Bildraum und die ursprüngliche Skalierung kann die Änderung anteilig in Bezug auf die Ausgangsamplitude als Zu- und Abnahme dargestellt werden. Zur Demonstration des Potentials der Curvelet basierten Änderungserkennung werden drei Anwendungsfälle aus dem Krisenkontext vorgestellt: Überflutung, Waldbrand, Erdbeben. In allen drei Fällen lässt sich die von der Katastrophe betroffene Fläche eindeutig von Flächen ohne Änderung abgrenzen. Die Interpretation dieser Änderungen ist jedoch ohne Zusatzwissen nicht möglich. Eine Verschneidung der Ergebnisse der Änderungserkennung mit bestehenden Geoinformationen hingegen liefert eine verlässliche Datengrundlage für die Organisation von Rettungskräften nach Naturkatastrophen.

www.schweizerbart.de
DOI: 10.1127/1432-8364/2010/0068
1432-8364/10/0068 $ 3.00

1 Introduction

Remote sensing products for disaster monitoring have to be fast and reliable. In most cases the coordinators do not have the time to wait for the next sunny day to acquire cloudless optical satellite images of the catastrophe. Radar sensors share the advantage to operate almost independently of weather and illumination, so that SAR images can be acquired in spite of a cloudy sky and even by night. Each illuminated object produces a certain SAR signature in the image. As the signatures of several objects overlay and interfere in fine-structured areas, a classification on SAR images is very complicated. Hence, the idea is not to classify single SAR images, but to identify changes between two image acquisitions before and after a natural disaster. In regions not affected by the impact, the radar signatures remain constant. Changes on the real objects mostly cause changes in the corresponding signatures, so that the affected regions can clearly be delineated. If the geometric properties of the images are held constant by using repeat orbit acquisitions, the only problem is the handling of the SAR inherent radiometry with its deterministic multiplicative noise-like component: speckle. Speckle is caused by the coherent sum of many distributed scatterers in one resolution cell (pixel). Hence, only individual pixels are affected whereas the structures of a scene joining an arbitrary number of individual pixels to geometric primitives e. g., lines, remain unchanged. Therefore, the comparison of two SAR amplitude images can be greatly simplified – because the false alarm rate is reduced – by comparing structures instead of single pixels. For this task a structure-based image description, called Curvelets, is utilized. The complex Curvelet coefficients, standing each for the strength of a linear feature in the image, allow us to compare and to manipulate structures in order to enhance a single as well as the difference between two SAR images. The developed change detection method runs automatically and delivers very robust results in a relatively short computation time. In contrast to the previous publications – reported in the following section – this article presents the theoretical background of the Curvelet-based change detection for the first time. Afterwards, the potential of the developed algorithm is validated for rapid mapping applications in the context of natural hazards. Three different disaster scenarios are considered: (1) The annual flood in the Caprivi stripe in Namibia (April 2009), which was the common test site for the DeSecure project; (2) Forest Fires on La Palma, Canary Islands (August 2009), where the Centre for Satellite Based Crisis Information (ZKI) of the German Aerospace Center has mapped the burned areas; (3) Damage on buildings in the city of Padang, Indonesia, after the earth quake of October 2009. For this test site reference information extracted visually from optical satellite images as well as some ground truth information, collected by several teams is available. Unfortunately, the ground truth data only covers single streets or building blocks.

The results of our change detection approach for SAR images are compared to the results of ZKI and the ground truth data respectively. In terms of the validation it is important to remember that the change detection on SAR data and the reference data – mainly extracted from optical satellite images – often show different results because of the different geometrical and radiometrical properties. Though, this study underlines the usefulness of SAR sensors as complementary data source in the context of satellite-based disaster management.

2 Related Work

Due to the geometric and radiometric properties of SAR images change detection gets more complicated – compared to optical data. Some basics of SAR change detection, advantages and constraints can be found in (Polidori et al. 1995), which reviews the fundamental approaches. (Scheuchl et al. 2009) distinguishes two different types of change detection: amplitude change detection and coherent change detection, exploiting the phase information. The latter one has been examined by (Wright et al. 2005). The method presumes a stable phase measurement, so that each incoherent region can be classified as changed. Regarding shorter wave lengths, even a repeat pass acquisition with a very short repetition

time (11 days in the case of TerraSAR-X) cannot assure coherence over natural cover. In the case of natural disaster monitoring, where reference images often date from several years ago coherence-based methods are not applicable because too much disturbing incoherence is caused by natural surfaces.

The amplitude-based change detection is better suited for the monitoring of diverse landscapes over a long period of time. (Derrode et al. 2003) and (Bouyahia et al. 2008) adopt a hidden and a sliding hidden Markov chain model respectively to select areas with changes in reflectivity even from images with different incidence angles. Although this method allows to process very large images and does not need additional parameter tuning, except the window size, according to the authors still a lot of research work has to be done to improve the preliminary results. Another idea starting with the fusion of several SAR images of different incidence angles and a coarse digital elevation model to a „superresolution" image is presented by (Marcos et al. 2006) and (Romero et al. 2006). Man-made objects, i. e., geometrical particularities that are not captured by the digital terrain model used for the orthorectification, are classified by their diverse appearance in the single orthorectified images due to the different acquisition geometries. So, seasonal changes in natural surroundings can easily be distinguished from changes in built-up areas. One disadvantage is the large number of different SAR images of the same area needed to generate the „superresolution" image.

In contrast to the precedent approach, (Balz 2004) needs a high resolution elevation model (e. g., acquired by airborne laser scanning) to simulate a SAR image with respect to the geometric appearance of the illuminated area. This simulated SAR image is subsequently compared to the real SAR data. The quality of the results is naturally highly dependent on the resolution of the digital elevation model and its co-registration to the SAR image. The influence of different surface materials is ignored so far. Although this method seems to be very promising, its application is still restricted to small-sized sample data. Another approach – based on radar measurements – has been published by (Molinier et al. 2007). This study focuses on the use of different polarimetric decompositions for the retrieval of several "polarimetric" features. The change detection consists in comparing the features extracted from the first image to the features extracted from the second image. As the feature extraction algorithm has to be trained in advance, this method is not suited for fully automatic data processing, e. g., in process chains. (Gamba et al. 2006) proposes a combined approach based on pixel values and geometrical features as well which are assumed to provide two uncorrelated sources of information. The goal is to utilize standard methods – implemented in all available SAR software products – to produce a rough pixel based change detection map and to extract edges of both amplitude images. The extracted features are subsequently compared to discriminate areas with changes from areas without changes and hence to stabilize the results of the pixel-based change map.

A very interesting approach using the Wavelet representation of a logarithmically scaled ratio image is given in (Bovolo & Bruzzone 2005). For the first time the influence of the speckle effect and several speckle reduction techniques on the change detection results is addressed. The originally one-dimensional Wavelet transform is extended to two dimensions in order to represent an image at different scales. The change detection results from coarser to finer scales are recombined to the final change map. Unfortunately, the procedure still is characterized by a high amount of manual interactions, e. g., trial-and-error threshold determination. Although the results are very promising, Wavelets do not seem to be the best representation for SAR images of urban areas (Schmitt et al. 2010b). Four different representations have been introduced into the same change detection procedure: Laplacian pyramid, Wavelets, Curvelets, and Surfacelets. While the Laplacian pyramid only distinguishes scales, Wavelets can distinguish horizontally and vertically aligned features. But, as most SAR signatures of urban areas are composed of linear elements of an arbitrary orientation, the Curvelet decomposition turns out to be the most effective way to describe urban scenes in SAR images (Schmitt et al. 2010b). Surfacelets are more suitable to

describe small-sized ellipse-like features, e. g., for car tracking purposes.

Curvelets for SAR image enhancement, structure extraction and change detection are considered for the first time in (Schmitt et al. 2009a). The core of this method is a special weighting function that is applied to the complex Curvelet coefficients of an image. Depending on the application different weighting functions are utilized. While the precedent publication mainly shows the potential of the Curvelet-based image understanding, (Schmitt et al. 2009b) focuses on change detection and its application to real SAR data over construction sites and mining areas. Since then, the weighting function as well as the scaling of the results has been improved several times in order to develop a fully automatic change detection approach independent of the image content. As the interpretation of the changes still is a very challenging task, multi-polarized SAR data is introduced as input data in (Schmitt et al. 2010a). By the help of the dual polarized High Resolution Spotlight mode of TerraSAR-X, the authors try to attach a physical meaning to the detected changes and to relate the derived changes in the scattering type to changes on real objects.

3 Change Detection with Curvelets

The Curvelet transform is designed to describe an image with singularities across straight lines, by a minimum number of coefficients (Candès & Donoho 1999). This fact shows the original purpose of the Curvelet transform: image compression. The basic element of the Curvelet theory is a linear feature, called Ridgelet, that is composed of a sine and a cosine component (see Figs. 1 & 2) represented by the real and the imaginary part of the corresponding coefficient. To describe an image effectively this basic element is transported to a wide range of scales, orientations and positions (Candès et al. 2005) and from now on called "Curvelet". In other words, each complex coefficient belongs to a certain Curvelet with a defined length, in a certain orientation and on a special position. The amplitude of the coefficient shows the strength of this linear

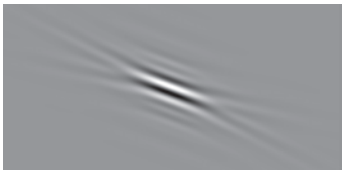

Fig. 1: Sine component.

Fig. 2: Cosine component.

feature in the original image. The value of one single pixel is thus calculated as sum of the contributions of all Curvelets in the image.

Transporting this theory to SAR images, clear structures in the image are always characterized by high coefficient amplitudes. In other words, the lower coefficients can be omitted without loss of structures. Former studies examine several types of weighting functions and different methods to adapt the function parameters to the image content. The results have already been submitted for publication. In short, the described image enhancement algorithm is based on a weighting function that is automatically adapted to the image content and then applied to the Curvelet coefficients of a SAR image. In terms of describing multiplicative speckle noise by an additive image representation, the SAR amplitudes have to be scaled logarithmically before the Curvelet transform is done. After weighting the coefficients and the inverse transform, the image is brought back to the original scaling by an exponential function.

The Curvelet-based change detection algorithm for already co-registered images exploits the following mathematical relations:

$$L_{x,y} = \sum_{i=1}^{n} C_i \cdot k_i \tag{1}$$

The logarithmized SAR amplitude $L_{x,y}$ found at position x, y in the image forms out of the sum over all Curvelets C_i multiplied with

the corresponding complex coefficients k_i. To detect changes in the radar amplitude the amplitude difference $D_{x,y}$ is calculated.

$$D_{x,y} = L_{2_{x,y}} - L_{1_{x,y}} \tag{2}$$

To express this relation via the Curvelet Coefficients, Eq. (1) is inserted into Eq. (2). As the input images share the same size, they share also the same number n of Curvelets. Therefore, the decomposition in scales, orientations and positions of the first image is consistent with the decomposition of the second image, i. e., the variable C_i stays constant while k_i varies depending on the image content.

$$D_{x,y} = \sum_{i=1}^{n} C_i \cdot k_{2i} - \sum_{i=1}^{n} C_i \cdot k_{1i} = \sum_{i=1}^{n} C_i \cdot (k_{2i} - k_{1i}) \tag{3}$$

In a nutshell, the images are compared by differentiating the corresponding Curvelet coefficients. An overview to the method is given in the flow chart in Fig. 3. The input images have to be co-registered in advance. In the case of TerraSAR-X data, the geocoding based on the science orbit information is sufficient. For practical use, the input images should be *Enhanced Ellipsoid Corrected* (*EEC*) products. Then, no further pre-processing is necessary. After the logarithmic scaling the Curvelet transform is performed. The differentiation of the Curvelet coefficients follows. To suppress clutter the image enhancement algorithm is applied to the coefficient differences before the difference image is transformed back to the spatial domain and scaled exponentially. The pixel values of the resulting difference image correspond to the relative changes $R_{x,y}$ in the SAR amplitudes, i. e., a relative increase by a certain percentage, see Eq. (4).

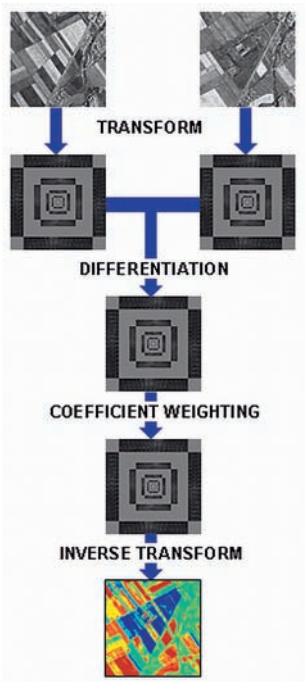

Fig. 3: Flowchart of the Curvelet-based change detection approach.

$$R_{x,y} = \left(e^{|Dx,y|} - 1\right) \cdot sign(D_{x,y}) \tag{4}$$

The sign of the differences gives the direction of the increase. While positive difference indicate an increase from the first to the second image, negative differences stand for an increase from the second to the first image. The exponential function is subsequently applied to the absolute value of the differences, which implies that every difference is seen as increase either from the first to the second image or the other way round. That's the reason why both increases and "decreases" of more than 100% can appear in both directions. At least the results of the exponential function are reduced by their minimum value, i. e., 1, so that the $R_{x,y}$ directly refers to the relative increase in the radar amplitude. The adoption of relative changes again accommodates the multiplicative nature of SAR images.

Mapping the increase and the decrease in the SAR amplitudes of single polarized images, allows to delineate regions that are characterized by this behavior, but it does not allow any interpretation of the mapped change. To explain what happened to the illuminated objects it is necessary to consult further data sources, e. g., a land cover classification or a building mask etc. One essential problem in the fusion of different data sources is still the coregistration of images having varying acquisition geometries, e. g., SAR data and optical data. Hence, our future work primarily will concentrate on the inclusion of polarimetric SAR data as purely SAR-based approach,

in order to attach the changes to certain scattering types. The knowledge about the change in the scattering geometry might help to interpret the change on the illuminated object and bear unknown potentials of SAR sensors.

4 Flood in Namibia

As common test site for the DeSecure project the Caprivi basin in the Caprivi stripe belonging to Namibia (Africa) was chosen. The annual flood reached very high water levels in the year 2009. the first SAR image has been taken during the flood in April (Fig. 4). The second image – seen as the pre-disaster acquisition – has been acquired in September after the flood (Fig. 5). Dark regions show very smooth surfaces where the incoming microwaves are scattered away from the sensor, e. g., calm water or pavement. By comparing the two TerraSAR-X Spotlight images with a ground pixel spacing of 1.75 m visually, we perceive large black regions in Fig. 4, showing the flooded areas, whereas in Fig. 5 the black pixels are restricted to the river and some roads. Flooded vegetation, i. e., flooded forests causes a higher backscattering. The trunks of trees enclosing a perpendicular angle with the water surface form a diplane scatterer that increases the backscattering of the whole area. In Fig. 4 the forested region on the top right – presumably flooded – appears brighter than in Fig. 5. Considering the Curvelet-based change detection, we have to take into account that the result is a change map instead of a water mask. Therefore, areas that are flooded in both images, e. g., the river, are not reported as change. As input for the change detection algorithm we use the enhanced ellipsoid corrected products in the radiometrically enhanced type.

Fig. 7 depicts the detected changes from the "pre-disaster" image to the image acquisition during the flood. The changes are colored according to the legend on the right. Changes of more than one hundred percent are not further distinguished. Green regions mark areas with no or only minor changes. Red colors mark an increase in the backscattering. In the imaged region this effect is mainly caused by flooded vegetation showing a high diplane scattering. Blue refers to a decrease in the backscattering amplitude which corresponds to recently flooded regions. As expected, only minor changes are indicated over the river and the road crossing the river. In comparison to the reference water mask, derived by the DeSecure project using thresholding methods on the backscattered intensity, the blue regions of the Curvelet-based change detection fit the flooded regions in Fig. 6. One larger region left in the middle that is reported flooded in Fig. 6 is marked in red in Fig. 7 because we find flooded vegetation there that causes an increase in backscattering. Having a closer look

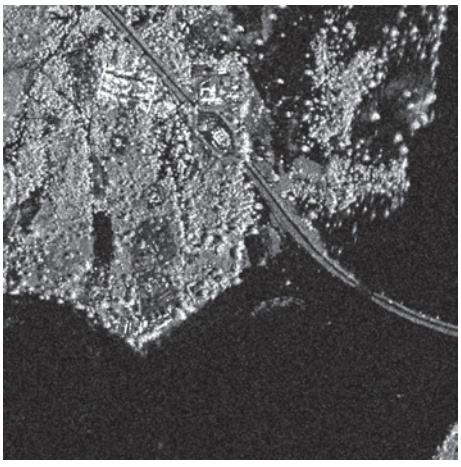

Fig. 4: Subset of TerraSAR-X Spotlight acquisition during the flood (06.04.2009).

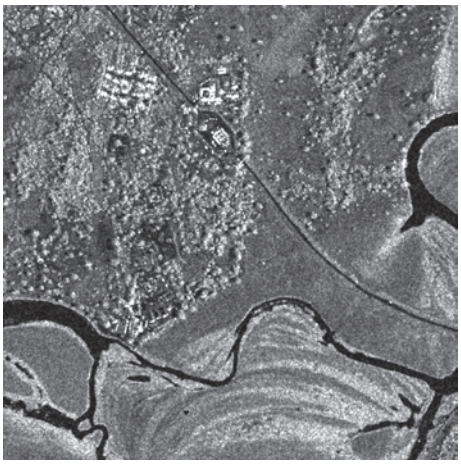

Fig. 5: Subset of TerraSAR-X Spotlight acquisition after the flood (07.09.2009).

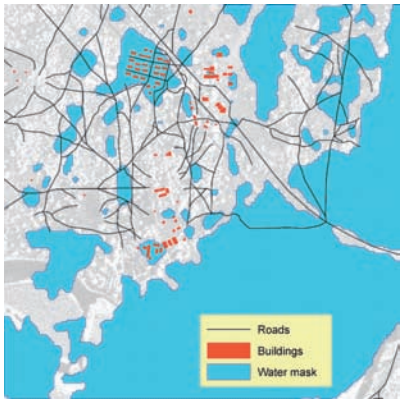

Fig. 6: Reference data: roads and buildings from Quickbird imagery, watermask from TerraSAR-X ScanSAR (11.04.2009).

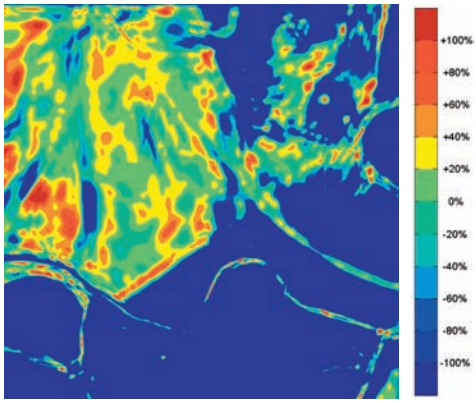

Fig. 7: Relative change of radar amplitude from 07.09.2009 (after the flood) to 06.04.2009 (during the flood), colored according to the colorbar on the right.

on both Figs. 6 and 7 we see many details that differ on the top left of the subset whereas the results near the river coincide very well. There are two simple reasons for this behavior. Firstly, the reference data is not ground truth data. As it is derived by simple amplitude thresholding of a TerraSAR-X ScanSAR scene and subsequently manually corrected, it only covers open water surfaces, i. e., flooded vegetation cannot be identified. Secondly, the ScanSAR image has been acquired five days later than the Spotlight images. Due to the very flat landscape, even a small deviation in water level causes large laminar changes in the flooded areas.

5 Forest Fires on La Palma

The second application of the Curvelet-based change detection approach is the mapping of burnt forest areas. The situation has been de-

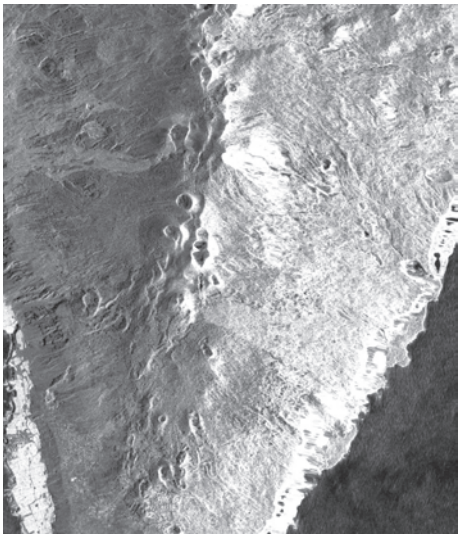

Fig. 8: Subset of TerraSAR-X Stripmap image before the forest fires (13.12.2007).

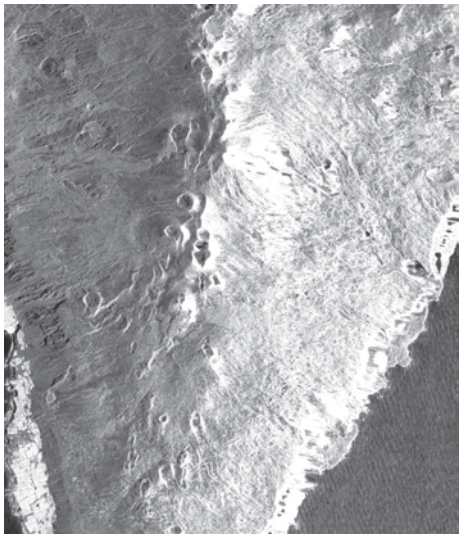

Fig. 9: Subset of TerraSAR-X Stripmap image after the forest fires (09.08.2009).

scribed by ZKI as follows: "Several forest fires occurred between July 31, 2009 and August 3, 2009 on the Canary Island of La Palma, Spain. 30 houses and several vineyards were destroyed. More than 4000 residents were evacuated from the area on August 1, 2009 (ZKI 2009a). As input for the Curvelet-based change detection we use TerraSAR-X radiometrically enhanced Stripmap products with a pixel spacing on ground of 2.75 m (EEC). The image in Fig. 8 shows the pre-disaster landscape on 13.12.2007. In Fig. 9 the post-disaster image dating from 9.8.2009 is depicted. The visual comparison delivers almost no changes, except on the ocean's surface on the bottom right.

In contrast to that the Curvelet-based change detection clearly delineates the burnt regions via the relative change in the backscattering amplitude (see Fig. 11). The reference map by ZKI is depicted in Fig. 10 and explained as follows: "The map shows the burnt areas as well as the locations of active fires between July 31, 2009 and August 3, 2009. The burnt areas were derived through the analysis of two Spot 5 scenes (pre disaster: 30/07/2007, post disaster: 07/08/2009). The locations of active fires were automatically derived from MODIS data" (ZKI 2009a). Although the reference again shows the situation at another time than the TerraSAR-X acquisition the burnt areas from Fig. 10 coincide very well with the regions showing an increase in backscattering in Fig. 11. The reason for this increase lies in the change of the scattering mechanism. While the leafy crowns of trees cause a high volume scattering – high values in the HV polarization and low values in both the HH and the VV polarization – the bare soil and the nude trunks respectively show high surface and diplane scattering, that means higher values in HH and VV. The TerraSAR-X images acquired in the HH polarization subsequently should report an increase in backscattering over burnt areas. Why the large area in the middle right that is marked as burnt in the reference map only is reported as minor change in Fig. 11, cannot be explained on the actual information basis. The effect on radar images highly depends on the change of the surface roughness of the illuminated areas caused by the fire. The use of multi-polarized radar data would help to identify the underlying scattering mechanisms instead of taking assumptions as hitherto. This could give a deeper insight to the type of forest before the fires and the degree of destruction after the fires.

6 Earthquake in Padang

The third example concerns the detection of damaged buildings in dense city centers. "On September 30, 2009, a severe earthquake took

Fig. 10: Reference data, visually digitized out of optical satellite image (ZKI 2009a).

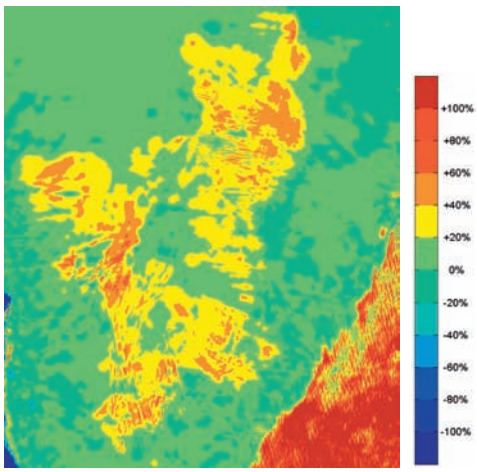

Fig. 11: Relative change of radar amplitude 13. 12. 2007 – 09. 08. 2009, according to colorbar.

place in the Indian Ocean with a magnitude of 7.9 and several aftershocks. The epicentre was registered about 50 km north-eastern of Padang in a depth of 85 km. Heavy shocks caused the collapse of many buildings and bridges, fires broke out and major parts of the technical infrastructure failed. More than 770 people died, much more than 2100 are injured (information of October 2, 2009). The International Charter on Space and Major Disasters was triggered to provide post-disaster satellite imagery for damage mapping and to support the aid response" (ZKI 2009b). A pre-disaster acquisition in the standard high resolution Spotlight mode dating from 21.11.2007 was available. The post-disaster image has been acquired in an experimental mode with the double pulse repetition frequency (PRF) and therefore possesses an increased azimuth resolution. In order to achieve equally-sized pixels on ground (1.25 m × 1.25 m) two different processing types in the geocoding step are utilized for image comparison. The first image (Fig. 12) with a minor azimuth resolution is processed as spatially enhanced product with a reduced accuracy in the radiometry, whereas the second image (Fig. 13) with a higher azimuth resolution is processed as radiometrically enhanced product with a reduced spatial resolution. The effects of the different acquisition modes and pre-processing steps are a higher noise level in Fig. 12 and a higher level of detail in Fig. 13. Despite these discrepancies in the input images, the automatic change detection delivers respectable results, see Fig. 15.

In order to enable the operator to attach single small-sized changes to objects, it is overlaid with the building mask that has been extracted from optical satellite imagery of IKONOS by (Taubenböck et al. 2009). Many changes – visible near the river – presumably refer to boats or pontoons. Presuming that all other mapped changes belong to buildings, we perceive striking deviations that result from the different image acquisition geometries of radar and optical data. The images should have been coregistered using the same high resolution surface model to avoid these effects. Although this inconsistence is negligible for our coarse validation, it has to be taken into account for real disaster applications. As reference information we use the damage assessment produced by (ZKI 2009b) which is described as follows: "Destroyed and damaged structures were derived by analyzing information provided by the Indonesian Disaster Management Authority (BNPB), from post-disaster Quickbird imagery acquired on October 3, 2009 (ground resolution 0.6 m) and from field data. The damage assessment is incomplete and in some cases inaccurate due to cloud cover and the difficulty to identify partly damaged buildings from bird's perspective"

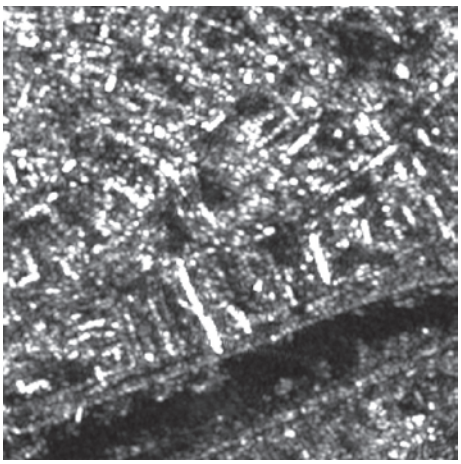

Fig. 12: Subset of TerraSAR-X Spotlight image, PRF 150 Mhz, spatially enhanced, pixel spacing 1.25 m (21. 11. 2007).

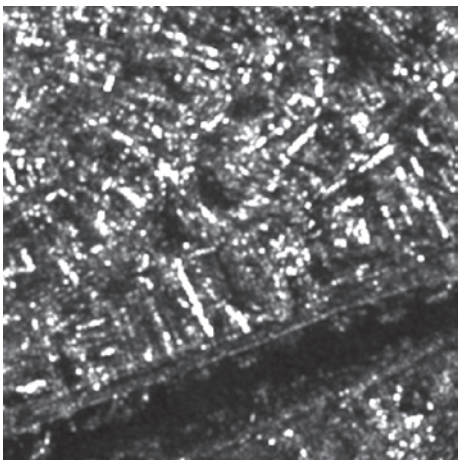

Fig. 13: Subset of TerraSAR-X Spotlight image, PRF 300 Mhz, radiometrically enhanced, pixel spacing 1.25 m (03. 10. 2009).

Fig. 14: Reference data, including streets and potentially damaged buildings: red (according to building structure survey) and yellow (on building characteristics derived from satellite imagery).

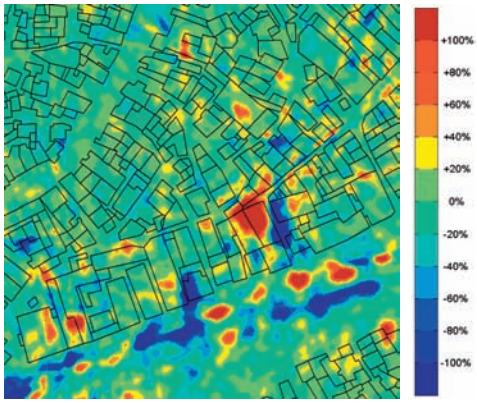

Fig. 15: Relative change of radar amplitude 07. 09. 2009 – 06. 04. 2009 and building mask from IKONOS imagery (Taubenböck et al. 2009).

(ZKI 2009b). Comparing the change detection results in Fig. 15 to the damage map in Fig. 14, only few sure coincidences are visible. Beside the incompleteness of the reference map, again the image acquisition geometry plays an important role. As the parallel projection in the case of optical scanning sensors is very similar to an orthogonal projection due to the large distance to the imaged objects, mostly roofs and nearly no facades are visible. In contrast the range projection of radar sensors reproduces roofs and facades as well. Hence, while optical sensors only reveal changes on nearly horizontal planes, i. e., ground or roofs, radar sensors show a high capability to map even changes on the buildings facades. Unfortunately, without any prior information the radar change detection results are only of limited value, because changes on natural surfaces cannot be distinguished from changes on man-made objects. But, this new technique enables to delineate areas with distinct changes to support the decision if a building that has been classified "potentially damaged" from pre-disaster analysis or optical satellite data is actually damaged or not. To conclude this example, radar information might not replace optical sensors and in-situ surveys, but it is a complementary tool to get reliable change information over large areas in a very short period of time and independent of weather, daylight or the accessibility of the injured city.

7 Conclusion

In this article we present a new change detection technique based on the Curvelet transform. This approach requires two or more coregistered SAR amplitude images. Changes in the SAR amplitudes over a certain period of time are captured as increase or decrease relative to the preceding amplitude values. Of course, the change detection approach can only detect changes present in the SAR amplitude data. Additionally, the size of the changes to be mapped must be superior to the pixel size, which was true for the chosen examples: flooded regions, burnt areas after forest fires, damaged buildings after an earthquake. The approach delivers robust and quasi noise-free results over natural landscapes as well as over urban environments. Validating urban scenes we have to consider the reference data source. Changes in the SAR image are always caused by changes on the imaged objects, but those are not always captured by other data sources used as reference, e. g., optical satellite data. And though the quantitative validation for large area applications is nearly impossible due to the lack of suitable reference data, the qualitative validation proved the reliability of the detected changes. The interpretation of the mapped changes is still topic to our research. The future focus lies on the exploitation of multi-polarized SAR data in terms of inter-

preting changes to objects by changes to the scattering mechanism. Another aim will be the fusion with pre-disaster optical image information in order to support human operators in interpreting the results of the SAR change detection, e. g., by the help of vulnerability maps or buildings masks.

References

Balz, T., 2004: SAR simulation based change detection with high-resolution SAR images in urban environments. – International Archives of Photogrammetry, Remote Sensing and Spatial Information Sciences **35** (B7): 472–477.

Bouyahia, Z., Benyoussef, L. & Derrode, S., 2008: Change detection in synthetic aperture radar images with a sliding hidden Markov chain model. – Journal of Applied Remote Sensing **2** (1).

Bovolo, F. & Bruzzone, L., 2005: A Detail-Preserving Scale-Driven Approach to Change Detection in Multitemporal SAR Images. – IEEE Transactions on Geoscience and Remote sensing **43** (12): 2963–2971.

Candès, E.J. & Donoho, D.L., 1999: Curvelets – a surprisingly effective nonadaptive representation for objects with edges. – Curve and Surface Fitting. Innovations in Applied Mathematics, Vanderbilt University Press, Saint-Malo (France): 105–120.

Candès, E.J., Demanet, L., Donoho, D.L. & Ying, L., 2005: Fast Discrete Curvelet Transforms. – Multiscale Modeling and Simulation **5:** 861–899.

Derrode, S., Mercier, G. & Pieczynski, W., 2003: Unsupervised Change Detection in SAR Images Using a Multicomponent HMC model. – Analysis of multitemporal remote sensing images. World Scientific Publishing Corporation: 16–18.

Gamba, P., Dell'Acqua, F. & Gianni Lisini, G., 2006: Change Detection of Multitemporal SAR Data in Urban Areas Combining Feature-Based and Pixel-Based Techniques. – IEEE Transactions on Geoscience and Remote Sensing **44** (10): 2820–2827.

Marcos, J.-S., Romero, R., Carrasco, D., Moreno, V., Valero, J.L. & Lafitte, M., 2003: Implementation of new SAR change detection methods: superresolution SAR change detector. – Journal for Photogrammetry and Remote Sensing **57:** 327–345.

Molinier, M., Laaksonen, J., Rauste, Y. & Hame, T., 2007: Detecting changes in polarimetric SAR data with content-based image retrieval. – IEEE Geoscience and Remote Sensing Symposium.

Polidori, L., Caillault, S. & Canaud, J.-L., 1995: Change detection in radar images: methods and operational constraints. – IEEE Geoscience and Remote Sensing Symposium: 1529–1531.

Romero, R., Marcos, J.-S., Carrasco, D., Moreno, V., Valero, J.L. & Lafitte, M., 2006: SAR Superresolution Change Detection for Security Applications. – ESA-EUSC Image Information Mining for Security and Intelligence, Torrejon air base, Madrid, Spain: on CD.

Scheuchl, B., Ullmann, T. & Koudogbo, F., 2009: Change Detection using High Resolution TERRASAR-X Data: Preliminary Results. – International Archives of Photogrammetry, Remote Sensing and Spatial Information Sciences **38** (1-4-7/W5): on CD.

Schmitt, A., Wessel, B. & Roth, A., 2009a: Curvelet Approach for SAR Image Denoising, Structure Enhancement, and Change Detection. – International Achives of Photogrammetry, Remote Sensing and Spatial Information Sciences **38** (3/W4): 151–156.

Schmitt, A., Wessel, B. & Roth, A., 2009b: Curvelet-based change Detection for man-made Objects from SAR Images. – IEEE Geoscience and Remote Sensing Symposium: 1059–1062.

Schmitt, A., Wessel, B. & Roth, A., 2010a: Introducing Partial Polarimetric Layers into a Curvelet-based Change Detection. – 8th European Conference on Synthetic Aperture Radar: 1018–1021.

Schmitt, A., Wendleder, A., Wessel, B. & Roth, A., 2010b: Comparison of Alternative Image Representations in the Context of SAR Change Detection. – IEEE Geoscience and Remote Sensing Symposium: on CD.

Taubenböck, H., Goseberg, N., Setiadi, N., Lämmel, G., Moder, F., Oczipka, M., Klüpfel, H., Wahl, R., Schlurmann, T., Strunz, G., Birkmann, J., Nagel, K., Siegert, F., Lehmann, F., Dech, S., Gress, A. & Klein, R. (2009): Last-Mile preparation for a potential disaster – Interdisciplinary approach towards tsunami early warning and an evacuation information system for the coastal city of Padang, Indonesia. – Natural Hazards and Earth System Sciences **9:** 1509–1528.

Wright, P., Macklin, T., Willis, C. & Rye, T., 2005: Coherent Change Detection with SAR. –European Radar Conference: 17–20.

ZKI, 2009a: Center for Satellite Based Crisis Information (ZKI) – Emergency mapping & Disaster Monitoring, a service of German Remote Sensing Data Center (DFD), 8.8.2009 www.zki.dlr.de/applications/2009/canaryislands/176_en.html (30.8.2010).

ZKI, 2009b: Center for Satellite Based Crisis Information (ZKI) – Emergency mapping & Disaster Monitoring, a service of German Remote Sensing Data Center (DFD), 1.10.2009 www.zki.dlr.de/applications/2009/indonesia/179_en.html (30.8.2010).

Address of the Authors:

Dipl.-Ing. Andreas Schmitt, Dr.-Ing. Birgit Wessel, Dipl.-Ing. Achim Roth, Deutsches Zentrum für Luft- und Raumfahrt (DLR), Deutsches Fernerkundungsdatenzentrum (DFD), Oberpfaffenhofen, Münchner Straße 20, D-82234 Weßling, Tel.: +49-8153-28-3341, -3307, -2706, Fax: -1445, e-mail: andreas.schmitt@dlr.de, birgit.wessel@dlr.de, achim.roth@dlr.de

Manuskript eingereicht: Juni 2010
Angenommen: September 2010